

SCALING CONCEPT WITH TEXT-GUIDED DIFFUSION MODELS

Anonymous authors

Paper under double-blind review

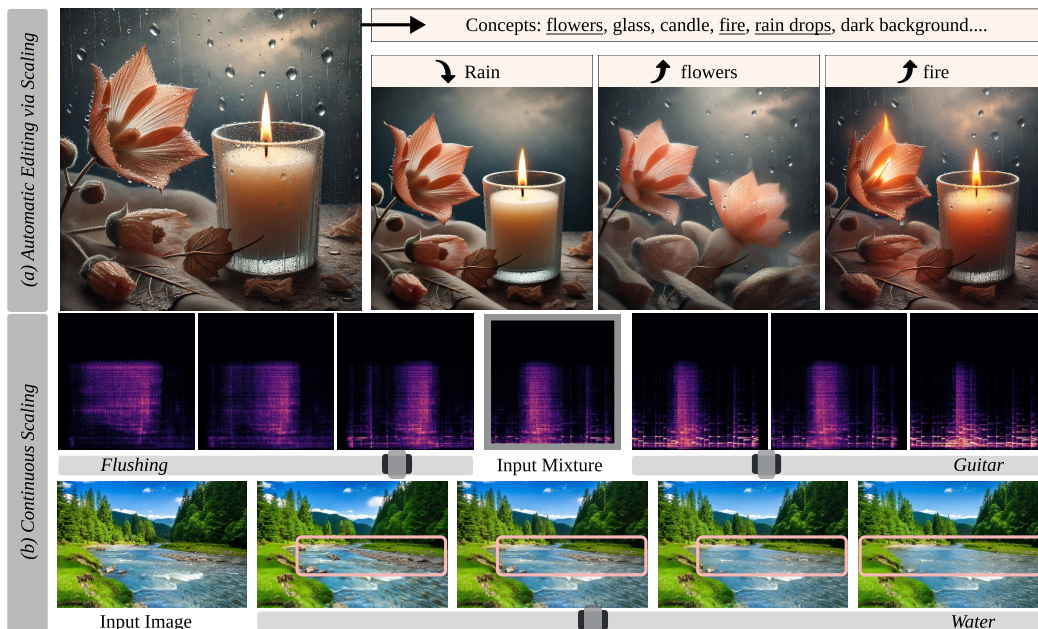


Figure 1: ScalingConcept provides two key functionalities: (a) Automatic Concept Suggestions: It leverages concepts automatically detected in the input, e.g., “fire,” “flowers,” and “rain” to generate scaling results. This enables automatic editing suggestions, offering users intuitive guidance on potential editing directions. (b) Continuous Concept Scaling: It supports slider-like functionality, allowing users to seamlessly adjust the prominence of a concept across both the audio and image domains.

ABSTRACT

Text-guided diffusion models have revolutionized generative tasks by producing high-fidelity content based on text descriptions. Additionally, they have enabled an editing paradigm where concepts can be replaced through text conditioning. In this work, we explore a novel paradigm: instead of replacing a concept, can we scale it? We conduct an empirical study to investigate concept decomposition trends in text-guided diffusion models. Leveraging these insights, we propose a simple yet effective method, **ScalingConcept**, designed to enhance or suppress existing concepts in real input without introducing new ones. To systematically evaluate our method, we introduce the *WeakConcept-10* dataset. More importantly, ScalingConcept enables a range of novel zero-shot applications across both image and audio domains, including but not limited to canonical pose generation and generative sound highlighting/removal.

1 INTRODUCTION

Derived from non-equilibrium thermodynamics, diffusion models (Sohl-Dickstein et al., 2015) have shown great success in content generation tasks. By defining a Markov chain that gradually injects

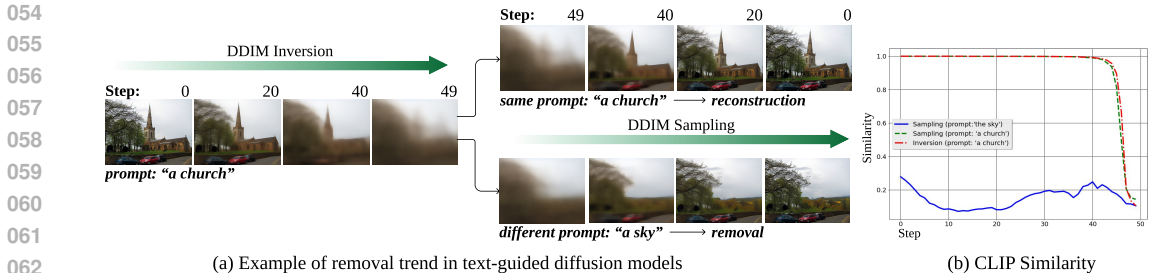


Figure 2: (a) Illustration of concept removal capability observed in the sampling process of text-guided diffusion models when conditioning on a conceptually different prompt compared to the inversion process. (b) We compute the CLIP zero-shot classification results between the classes [“a sky”, “a church”] and the reconstruction results at each inversion/sampling step (the total number of sampling step is 50), and report the classification accuracy of the class “a church”. It’s observed that the church object is removed from the removal branch even at the very early stages of sampling.

random noise into data and learning the reverse process, diffusion models generate new content from random noise in an iterative manner. This new generation paradigm has been applied to various domains, such as image generation (Nichol et al., 2022; Ramesh et al., 2022; Saharia et al., 2022; Rombach et al., 2022), video generation (Ho et al., 2022; Singer et al., 2023; Wu et al., 2022; Khachatryan et al., 2023; Guo et al., 2023; Chen et al., 2024; Brooks et al., 2024), and audio generation (Yang et al., 2023; Liu et al., 2023a; Huang et al., 2023b; Ghosal et al., 2023; Liu et al., 2023b; Huang et al., 2023a). Text-guided diffusion models, in particular, have garnered significant attention due to their ability to control content through natural language guidance.

The advent of text-guided diffusion models has enabled text-guided content editing. Several works (Hertz et al., 2023; Gal et al., 2022; Ruiz et al., 2023; Kumari et al., 2023; Brooks et al., 2023; Dhariwal & Nichol, 2021; Song et al., 2020; Mokady et al., 2023) have adapted diffusion models for this purpose. For instance, DreamBooth (Ruiz et al., 2023) fine-tunes a text-to-image diffusion model using a few images of an object paired with a text prompt c that contains the class information of the object. Null-text Inversion (Mokady et al., 2023) addresses the reconstruction error caused by DDIM Inversion (Song et al., 2020) in editing by updating the null-text embedding. LEDITS++ (Brack et al., 2024) improves the accuracy of text-guided editing and supports multiple simultaneous edits. These methods typically focus on addressing a long-standing editing challenge of replacing concepts, such as using an inversion prompt $c = “a dog”$ and an editing prompt $c' = “a swimming dog.”$ While replacement-based paradigms have achieved significant progress in enabling deterministic editing based on clearly defined prompts c' , they may fall short in scenarios where users are uncertain about how to specify c' . Additionally, certain editing effects are difficult to quantify through text prompts. For example, an instruction such as “a river with more water” does not provide an exact specification of the desired increase in water levels, leading to potential ambiguity. Such instructions may correspond to a range of variations in the outcome, as text prompts inherently lack the precision to represent these changes quantitatively.

In this work, we explore a new paradigm beyond the common editing pipeline, which typically involves replacing one concept with another. Instead, we focus on the research question: *Can we edit the concept continuously without any extra human efforts on specifying a target?* Specifically, this requires methods capable of isolating concept representations from real input and performing targeted edits on these representations. A surprising finding partially answers this question: text-guided image diffusion models, such as Stable Diffusion (Rombach et al., 2022), exhibit the ability to remove concepts through text prompts. As shown in Figure 2, applying the prompt $c = “a church”$ during inversion and the forward prompt $c' = “a sky”$ unexpectedly removes the church, while inpainting its region with the neighboring regions. We further investigate this phenomenon by examining its scalability and modality agnosticism, as detailed in Section 3.2. Through empirical analysis, we observe that the concept removal trend exists on a scalable level, and is not limited to a single modality (both image and audio), proving to be modality-agnostic.

Motivated by the concept removal and reconstruction branches demonstrated in Figure 2, we propose to model the difference between these two branches as a proxy for representing the concept itself,

introducing our method, ScalingConcept. Specifically, given the concept c to be scaled, we apply an inversion technique using text-guided diffusion models to obtain the concept-sensitive latent variable x_T . During the sampling process, we model the difference between the noise predictions of the reconstruction and removal branches. A scaling factor is integrated to control the modeling process across different diffusion time steps. Additionally, we introduce a noise regularization term to better balance the fidelity and concept scaling. As shown in Figure 1, our method specializes in the pipeline by modifying the existing concepts in the input, providing editing suggestions without specifying new concepts. Also, by scaling the concept, our method demonstrates a continuous editing capability, such as gradually increasing the water level or making stones disappear progressively. Additionally, our approach interacts solely with the input and output of diffusion models, avoiding intricate modifications to the network’s architecture. This design ensures that our approach can be seamlessly applied to diffusion models across various modalities, including audio. Experiments on the public editing dataset TEdBench (Kawar et al., 2023) and our *WeakConcept-10* dataset show that our method outperforms baseline methods in concept scaling, with detailed analysis of the effect of different components.

Interestingly, our zero-shot ScalingConcept method unlocks several downstream applications (as shown in Figure 1) without additional cost. Scaling up a concept standardizes its representation while scaling down tends to remove it. In the image domain, this enables tasks, *e.g.*, canonical pose generation, object stitching, weather manipulation, and creative enhancement. Scaling up adjusts non-standard object poses, completes stitched objects, and harmonizes them with the background. It also allows for altering weather effects, such as deraining or dehazing. In the audio domain, we achieve sound highlighting by amplifying text-indicated sounds and suppressing others, as well as generative sound removal by decomposing audio mixtures into individual components.

In all, our contributions can be summarized as follows:

- We formulate the research question on *concept scaling* and propose ScalingConcept, which has two features: (1) editing the inherent concepts within the input, reducing the effort required for laborious specification of a target, and (2) continuously scaling the concepts along a spectrum, from removal to enhancement.
- To quantitatively validate the effectiveness of ScalingConcept, we introduce a new dataset, *WeakConcept-10*, specifically designed to benchmark concept scaling. We also evaluate its concept suppression capability on the TEdBench (Kawar et al., 2023) dataset. Experimental results demonstrate that our training-free ScalingConcept outperforms baselines across multiple metrics.
- The proposed ScalingConcept showcases its versatility through a variety of zero-shot applications across image and audio domains, such as canonical pose generation, object stitching, weather manipulation, sound highlighting, and generative sound removal, all achieved without additional training. This approach serves as a valuable complement to existing replacement-based editing methods.

2 RELATED WORKS

2.1 TEXT-GUIDED DIFFUSION MODELS

Text-guided diffusion models have set a new standard for realistic content generation across multiple domains, including images (Nichol et al., 2022; Ramesh et al., 2022; Saharia et al., 2022; Rombach et al., 2022), videos (Ho et al., 2022; Singer et al., 2023; Wu et al., 2022; Khachatryan et al., 2023; Guo et al., 2023; Tang et al., 2024; Brooks et al., 2024), and audio (Yang et al., 2023; Liu et al., 2023a; Huang et al., 2023b; Ghosal et al., 2023; Liu et al., 2023b; Huang et al., 2023a). A major factor contributing to their success is the deep integration of language understanding into the content generation process. For instance, the GLIDE model (Nichol et al., 2022) introduced text-conditional diffusion models that enable controlled image synthesis, while DALL-E 2 (Ramesh et al., 2022) employed a two-stage approach leveraging joint CLIP embeddings (Radford et al., 2021) to capture semantic information from text inputs. Similarly, Imagen (Saharia et al., 2022) showcased the efficacy of large pre-trained language models like T5 (Raffel et al., 2020) in encoding text prompts for image generation tasks. Latent Diffusion Models, such as Stable Diffusion (Rombach et al., 2022), further optimized the diffusion process by performing it in the latent space, enhancing both efficiency and

162 generation quality. The success observed in the image domain has extended to other modalities. For
 163 instance, methods like the Video Diffusion Model (VDM)(Ho et al., 2022), Make-A-Video(Singer
 164 et al., 2023), AnimateDiff (Guo et al., 2023), and VideoCrafter (Chen et al., 2023) adapted these
 165 models to generate videos from text. In the audio domain, works such as AudioLDM (Liu et al.,
 166 2023a), Make-An-Audio (Huang et al., 2023b), and TANGO (Ghosal et al., 2023) have achieved
 167 promising results, illustrating the adaptability of diffusion models to various modalities. The success
 168 of these models across domains is underpinned by their ability to learn robust text-to-modality
 169 associations, proving that textual concepts can be effectively mapped to different types of content. In
 170 our work, we build upon these associations, introducing a novel approach to leverage text-guided
 171 diffusion models across multiple modalities for the purpose of concept scaling.

172 2.2 TEXT-GUIDED EDITING WITH DIFFUSION MODELS

174 Text-guided content editing using diffusion models has seen rapid development in recent years.
 175 Approaches such as DreamBooth (Ruiz et al., 2023), Null-text Inversion (Mokady et al., 2023), and
 176 InstructPix2Pix (Brooks et al., 2023) have introduced techniques to fine-tune and control diffusion
 177 models for specific editing tasks. These works focus on replacing or modifying objects within an image
 178 by manipulating inversion techniques and null-text embeddings. For instance, DreamBooth (Ruiz
 179 et al., 2023) allows for text-guided personalization of diffusion models by fine-tuning them with
 180 a small number of images. Null-text Inversion (Mokady et al., 2023) resolves issues related to
 181 reconstruction errors when editing specific concepts through prompt-guided inversion. *InfEdit (Xu
 182 et al., 2023) introduces an inversion-free editing framework that accelerates the editing process while
 183 ensuring faithful results. PnP Inversion (Ju et al., 2024) leverages the source diffusion branch to
 184 correct inversion deviations, enhancing the accuracy of edits.* A recent method LEDITS++ (Brack
 185 et al., 2024) provides a novel inversion approach to produce high-fidelity results with a few diffusion
 186 steps and supports multiple simultaneous edits. PromptFix (Yu et al., 2024) enhances diffusion
 187 models by improving their ability to follow diverse, low-level image editing instructions, while
 188 FineMatch (Hua et al., 2024) introduces fine-grained evaluation for text-image alignment, focusing
 189 on mismatch detection and correction. *In contrast to these methods, which primarily focus on concept
 190 replacement, we explore a specific editing paradigm: concept scaling. This approach eliminates the
 191 need for explicitly defining instructions, enabling automatic editing suggestions for real-world inputs.*
 192 *Furthermore, it supports continuous editing for scenarios where target instructions are difficult to
 193 quantify, offering a more flexible and intuitive editing framework.*

194 3 METHOD

196 In this section, we first review the foundational concepts of text-guided diffusion models and diffusion
 197 inversion techniques in Section 3.1, which form the basis of our analysis. Next, we provide an
 198 empirical analysis of the trend of concept decomposition observed in text-guided diffusion models in
 199 Section 3.2. Finally, in Section 3.3, we introduce our novel approach, ScalingConcept, which allows
 200 flexible control over the strength of the target concept in real input data.

202 3.1 PRELIMINARY

203 **Text-guided Diffusion Models.** Text-guided diffusion models have gained significant attention for
 204 their success in generating realistic images, audio, and video from text prompts. Their key strength
 205 lies in accurately capturing text-to-X associations, where X refers to any modality. Taking an image
 206 as an example, the process typically begins using an autoencoder such as VQ-GAN (Esser et al.,
 207 2021) to project an input into a latent vector \mathbf{x}_0 . During diffusion, Gaussian noise is progressively
 208 added to the latent feature, resulting in a random noise vector \mathbf{x}_T . In the denoising phase, a noise
 209 prediction network ϵ_θ learns to estimate the noise added at each step. Text-guided diffusion models
 210 use a text condition \mathbf{c} , usually derived from text embeddings like CLIP (Radford et al., 2021), to
 211 guide the sequential denoising process. The learning objective is defined as:

$$212 \ell_{simple} = \|\epsilon - \epsilon_\theta(\mathbf{x}_t, \mathbf{c}, t)\|, \quad (1)$$

213 where ϵ is the Gaussian noise added at timestep t .

214 **Inversion Technique.** Inversion techniques are commonly used in generative models to enable the
 215 editing of real content (Xia et al., 2022; Gal et al., 2022; Mokady et al., 2023). Typical inversion

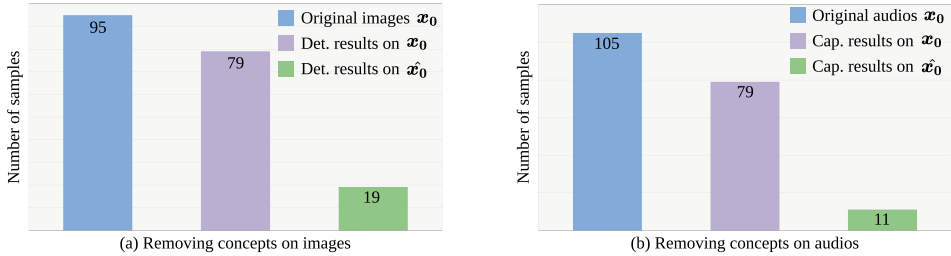


Figure 3: Analysis of the trend of concept removal. We erase target concepts from given images and audio clips using the proposed inversion and sampling process. We report the number of samples with target concepts before and after concept removal.

methods, such as DDIM inversion (Dhariwal & Nichol, 2021; Song et al., 2020), convert an input latent \mathbf{x}_0 into a noisy latent variable \mathbf{x}_T , which can then be used to reconstruct \mathbf{x}_0 or perform edits. Specifically, DDIM inversion leverages its deterministic sampling process:

$$\mathbf{x}_{t-1} = \sqrt{\frac{\bar{\alpha}_{t-1}}{\bar{\alpha}_t}} \mathbf{x}_t + \left(\sqrt{\frac{1}{\bar{\alpha}_{t-1}} - 1} - \sqrt{\frac{1}{\bar{\alpha}_t} - 1} \right) \epsilon_\theta(\mathbf{x}_t, \mathbf{c}, t), \quad (2)$$

with $\{\bar{\alpha}_t\}_{t=0}^T$ as a predefined noise schedule. This process iteratively denoises \mathbf{x}_T to recover \mathbf{x}_0 . Due to ODE formulation, it can be reversed, with small steps, to obtain the inversion (denoted as $f^{inv}(\mathbf{x}_t, \mathbf{c}, t)$):

$$\mathbf{x}_{t+1} = \sqrt{\frac{\bar{\alpha}_{t+1}}{\bar{\alpha}_t}} \mathbf{x}_t + \left(\sqrt{\frac{1}{\bar{\alpha}_{t+1}} - 1} - \sqrt{\frac{1}{\bar{\alpha}_t} - 1} \right) \epsilon_\theta(\mathbf{x}_t, \mathbf{c}, t), \quad (3)$$

thereby estimating the noisy latent \mathbf{x}_T from \mathbf{x}_0 . Starting with \mathbf{x}_T , the sampling process can be guided by arbitrary text conditions. However, DDIM inversion is limited by cumulative errors at each step, which deviate the path toward the correct latent noise. Several methods, such as DDPM inversion (Huberman-Spiegelglas et al., 2024) and ReNoise (Garibi et al., 2024), have been proposed to improve the inversion process.

3.2 EMPIRICAL ANALYSIS ON THE CONCEPT REMOVAL

Equation (3) and Equation (2) define a pair of destruction and reconstruction processes. In prior research, this framework has been successfully utilized for concept editing. Given an input \mathbf{x}_0 , the inversion process extracts the latent variable \mathbf{x}_T . The reverse process generates an edited output where the original concept c is modified to \tilde{c} , enabling various forms of editing such as object or style changes (e.g., “a photo of a dog” \rightarrow “a photo of a horse”). While previous work has focused on replacing the concept with a new one, our research asks a different question: can the existing concept be enhanced or suppressed?

We explore the first question through a case study illustrated in Figure 2. We perform an inversion with the prompt “a church,” which branches into two sampling paths: (1) using the same prompt, “a church,” to reconstruct the image as expected, and (2) using the prompt “a sky.” Interestingly, on the second path, the church is removed, and the vacated area is inpainted with content related to the surrounding context, even from the first sampling step. We hypothesize that this removal effect is due to the interplay between cross- and self-attention mechanisms in diffusion models. During inversion, the noise estimator ϵ_θ relies heavily on cross-attention to incorporate context from \mathbf{c} , leading to the strongest modification in regions associated with the concept c . However, during sampling, when the prompt “a sky” provides no useful context for reconstructing the church, self-attention becomes dominant, leading to the church’s removal.

Does the Concept Removal Trend Appear on Scale? To determine if the concept removal phenomenon is isolated or consistent across a broader dataset, we replicate the process from Figure 2 using more samples from the COCO (Lin et al., 2014) dataset. For each image \mathbf{x}_0 , we apply the DDIM inversion with the prompt “[class].” After obtaining the noisy latent variable \mathbf{x}_T , we use a

270 null prompt \emptyset for the sampling process to convert x_T back into an image \hat{x}_0 . Note that we use the
 271 null prompt for all images as a versatile solution for the removal branch. However, the null prompt
 272 can be automatically replaced, as described in Section 3.3. This process mirrors that in Figure 2,
 273 aiming to remove the concept of “[class]” from the input image. To assess whether the concept was
 274 successfully removed, we used Grounding DINO (Liu et al., 2023c) to detect the presence of the
 275 “[class]” object in both x_0 and \hat{x}_0 . The results, shown in Figure 3, indicate that the target concept
 276 corresponding to “[class]” is successfully removed in 80% of the images. This confirms that the
 277 concept removal capability exists at scale, rather than being limited to a single sample.

278 **Does the Concept Removal Apply to Other Modality?** To explore this, we conduct a similar
 279 experiment with audio. Using the AVE dataset (Tian et al., 2018), an audio event classification
 280 dataset containing clips from 28 sound classes, we randomly sampled 5 audio clips from each class.
 281 We employ AudioLDM 2 (Liu et al., 2023b) to perform the same process as in the image-based
 282 experiment. To determine whether the concept was removed from the original audio clip, we use
 283 EnCLAP (Kim et al., 2024), an audio captioning framework, to generate captions for both x_0 and \hat{x}_0 .
 284 We then check whether the word “[class]” appeared in the captions. As shown in Figure 3, the same
 285 trend of concept removal was observed in audio, despite its fundamentally different nature compared
 286 to images.

287 **Discussions.** From the empirical analysis above, we observe that starting from the same latent
 288 variable x_T obtained by inversion, we can define both a reconstruction branch and a removal branch.
 289 This implicitly suggests that text-guided diffusion models possess the ability to **extract a concept**.
 290 Building on these findings, an important research question emerges: can we control the divergence
 291 between these two branches to achieve concept scaling?

292 3.3 OUR METHOD: SCALINGCONCEPT

294 Motivated by the difference between the removal and reconstruction branches, we propose **Scal-**
 295 **ingConcept**, a method designed to decompose the concept from real input and scale it up or down,
 296 effectively enhancing or suppressing the corresponding representation in the input. Our method
 297 consists of the following steps:

298 **Step 0 (Optional): Concept Parsing.** To facilitate the scaling of embedded concepts in real-world
 299 inputs, an optional preliminary step involves parsing concepts from the input (*e.g.*, an image) using
 300 off-the-shelf vision-language models. The parsed concepts can then be leveraged to automatically
 301 construct the reconstruction and removal branches. In the removal branch, we utilize the null prompt
 302 as a baseline example, as described in the subsequent notation. Additionally, Figure 17 provides
 303 an analysis of replacing the null prompt with parsed non-c concepts, highlighting its impact on the
 304 editing process.

305 **Step 1: Generating Scaling Startpoint x_T .** Given a real input x_0 and a concept c to scale,
 306 represented by a text prompt such as “*fire hydrant*,” we use a pre-trained text-guided diffusion model
 307 ϵ_θ to perform sequential inversion functions as described in Equation (3):

$$308 \quad x_T = f^{inv}(x_0, c, 0) \circ \dots \circ f^{inv}(x_{T-1}, c, T - 1). \quad (4)$$

309 In our experiment, we use ReNoise Garibi et al. (2024) as the inversion technique.

311 **Step 2: Concept Scaling.** Starting from x_T , we define two prompts: the first is the text prompt c used
 312 during inversion, corresponding to the reconstruction branch, and the second is the null-text prompt
 313 \emptyset , representing the removal branch. The noise predictions from the two branches are denoted as
 314 $\epsilon_t^\emptyset = \epsilon_\theta(x_t, \emptyset, t)$ and $\epsilon_t^r = \epsilon_\theta(x_t, c, t)$, where the superscript r stands for reconstruction. We model
 315 the difference between these two branches by capturing the difference in their noise predictions.

$$316 \quad \hat{\epsilon}_t = \epsilon_t^\emptyset + \omega_t \cdot (\epsilon_t^r - \epsilon_t^\emptyset). \quad (5)$$

317 We introduce a scaling factor ω_t to control the magnitude of the difference at each step t . Note
 318 that when $\omega_t = 1$, Equation (5) degrades to the vanilla reconstruction branch. A value of $\omega_t < 1$
 319 suppresses the concept, while $\omega_t > 1$ enhances it. Intuitively, during the early steps of inference, the
 320 model captures coarse-grained details such as global structure and shape, whereas in the final steps, it
 321 focuses on refining high-frequency details (Si et al., 2024). To explore the impact of different designs
 322 for ω_t , we express it as $\omega_t = \omega_{base} * \beta(t)$, where ω_{base} controls the overall strength of scaling, and
 323

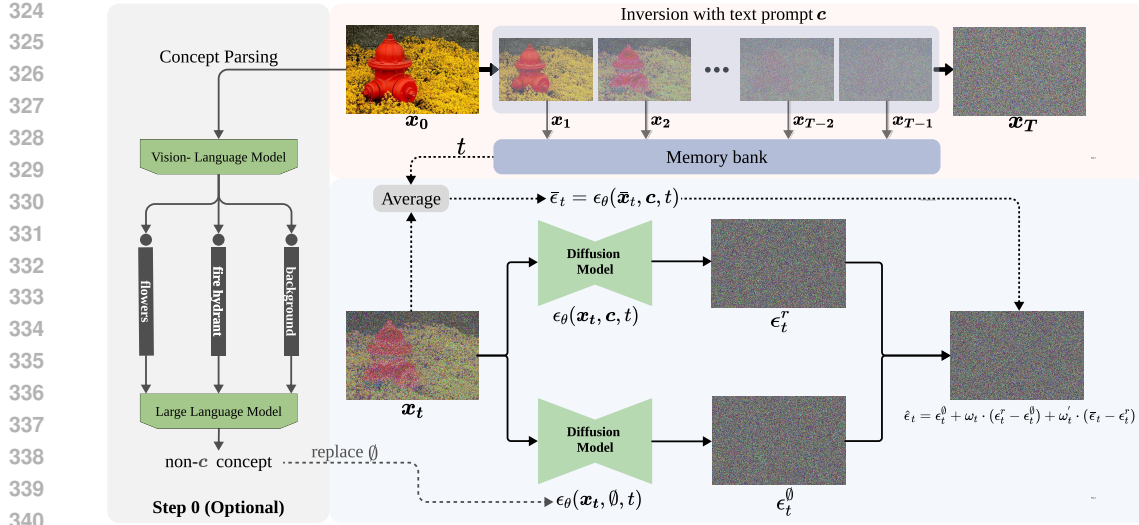


Figure 4: Overview of the ScalingConcept framework. Our method consists of three steps: 0) (Optional) Extracting the embedded concepts from the input by prompting off-the-shelf vision-language models, 1) extracting the latent variable from x_0 , and 2) constructing different sampling branches and modeling the difference between them.

$\beta(t)$ is a scheduling function within the range 0 to 1. We propose a dynamic schedule $\beta(t) = \left(\frac{t}{T}\right)^\gamma$, where γ controls the sharpness of the scaling. This approach supports three common schedules: 1) Constant ($\gamma = 0$), treats the difference equally across all steps, similar to classifier-free guidance in diffusion models. 2) Linear ($\gamma = 1$), reflects a linear change in the concept’s impact. 3) Non-linear ($\gamma \neq 0$ or 1), allows for dynamic adjustments of the concept’s influence, depending on the value of γ .

Noise Regularization. When ω_t is set to a very large value, the noise prediction $\hat{\epsilon}_t$ in Equation (5) can deviate significantly from the real input, leading to dissimilar content despite the concept being scaled—an undesired effect. Our goal is to scale the concept while preserving the context of the original input. To address this, we introduce a noise regularization term. At each timestep t , we retrieve the corresponding noisy latent generated during the inversion process from the memory bank. We combine this with the current noisy latent, adjust the noise predictions using an averaging operation, and then reintroduce them into Equation (6) using the same scaling factor. Additionally, since the forward noisy latents deviate further from the inversion latents in the later steps, we apply an early exit method to stop noise regularization when necessary. The regularized noise prediction is defined as:

$$\hat{\epsilon}_t = \epsilon_t^\theta + \omega_t \cdot (\epsilon_t^r - \epsilon_t^\theta) + \omega'_t \cdot (\bar{\epsilon}_t - \epsilon_t^r), \quad (6)$$

$$\omega'_t := \begin{cases} 0 & \text{if } t < t_{exit}, \\ \omega_t & \text{otherwise.} \end{cases} \quad (7)$$

In our experiment, t_{exit} is empirically set to 35, out of a total of 50 sampling steps.

4 EXPERIMENT

4.1 EXPERIMENTAL SETTINGS

WeakConcept-10 Dataset. To effectively test concept scaling, it is essential to have a dataset that supports the measurement of concept strength. However, evaluating whether a concept has been enhanced or suppressed in real inputs poses a significant challenge. To address this, we leverage Stable-Diffusion-3 (SD3) (Esser et al., 2024), a recently released and powerful text-guided image diffusion model, to generate images exhibiting weak concepts. We begin by selecting 10 categories that cover a diverse range of aspects, including *sofa*, *banana*, *cat*, *flower*, *Van Gogh*, *ship*, *Statue*

Table 1: Comparison of different methods for concept enhancement. Results are grouped by dataset: WeakConcept-10 and TEdBench (Kawar et al., 2023). Our method (ScalingConcept) achieves the best performance across multiple metrics.

Method	WeakConcept-10			TEdBench (Kawar et al., 2023)		
	FID ↓	CLIP (%) ↑	LPIPS ↓	FID ↓	CLIP (%) ↓	SR ↑ (%)
<i>Input</i>	313.4	26.9	-	-	27.3	-
Instruct Pix2Pix	312.0	27.8	0.312	322.1	25.5	38.4
LEDITS++	274.4	28.6	0.321	316.6	22.6	58.9
Ours	272.2	28.6	0.291	315.3	22.6	69.2



Figure 5: Qualitative comparison with baseline methods. We display the input images with weak concepts from our dataset, the enhanced results of two baseline approaches, and those of our ScalingConcept method. The concepts being scaled up are “cat,” “ship,” “sofa,” and “flowers”, arranged from top-left to bottom-right.

of Liberty, fruits, forest, and horse. For each category, we generate 10 images using the prompt “[class_name]” while setting the guidance scale to 1, ensuring that the generated images reflect weak representations of the target concept. As illustrated in Figure 18, the generated images display indistinct structures and missing details of the specified concept, making them suitable candidates for improvement through concept scaling. This dataset is particularly for evaluating the concept enhancing (scaling up) performance. We utilize three metrics to evaluate performance: CLIP score (Radford et al., 2021), FID (Heusel et al., 2017), and LPIPS (Zhang et al., 2018). The CLIP score assesses whether the target concept has been successfully enhanced, while FID evaluates the overall image quality after concept enhancement. Finally, LPIPS measures the perceptual similarity between the enhanced output and the original weak input.

TEdBench (Kawar et al., 2023) Dataset. We further evaluate the concept scaling-down performance using the public image editing dataset TEdBench (Kawar et al., 2023), which comprises 39 images from diverse categories. For each image, we specify a concept to be scaled down, as detailed in Table 3. To assess performance, we use FID to evaluate the overall image quality after scaling down the concept, CLIP score to measure whether the specified concept has been successfully scaled down, and Success Rate (SR) to quantify the percentage of images where the concept has been successfully scaled down. A common failure mode involves returning the original, unmodified image, which is considered unsuccessful.

4.2 MAIN COMPARISON

To evaluate the effectiveness of our ScalingConcept method, we compare it against Instruct Pix2Pix (Brooks et al., 2023), which enhances the concept by using the prompt “enhance the [concept]”. Additionally, we adapt another editing method, LEDITS++ (Brack et al., 2024), for our experiment. While LEDITS++ is capable of both adding and removing concepts, in our case, we use it to add the concept again, as the input already contains the concept, effectively simulating concept enhancement. The comparison results are presented in Table 1. Both LEDITS++ and our method achieve comparable concept strength, as indicated by similar CLIP scores. However, our method produces superior image quality, reflected by a lower FID score, while also preserving the original context of the input. This demonstrates the effectiveness of ScalingConcept in both enhancing the concept and maintaining image fidelity. For a qualitative comparison, see Figure 5, where our method clearly enhances the weak concept while preserving fine details in the image. Similarly, we evaluate the scaling-down

Table 2: Ablation studies of our method design. We set $\omega_{base} = 5$ for all experiments. We test the performance with various values of γ and examine the impacts of noise regularization and early exit.

Configuration	Noise Regularization	Early Exit	FID	CLIP (%)	LPIPS
$\gamma = 0$ (Constant)	✗	✗	232.9	28.6	0.397
$\gamma = 0.5$ (Non-linear)	✗	✗	238.6	28.7	0.380
$\gamma = 1$ (Linear)	✗	✗	242.0	28.7	0.368
$\gamma = 3$ (Non-linear)	✗	✗	258.1	28.5	0.324
$\gamma = 3$	✓	✗	282.6	28.5	0.260
	✓	✓	272.2	28.6	0.291

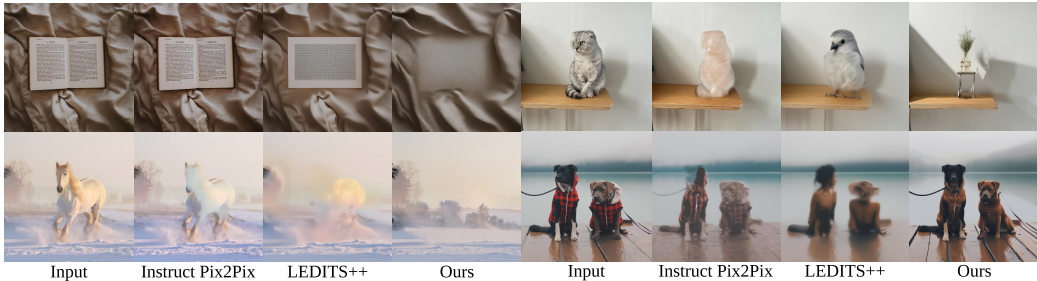


Figure 6: Qualitative comparison with baseline methods on concept scaling-down. We present the real input images from the TEdBench dataset alongside the scaling-down results of two baseline approaches and our ScalingConcept method. The concepts being scaled down are “open book,” “cat,” “horse,” and “checkered hoodies”, arranged from top-left to bottom-right.

performance, where the goal is to suppress the concept using the TEdBench dataset (Kawar et al., 2023). Our method achieves a lower FID score and a higher success rate (approximately 10% improvement) compared to the strong baseline LEDITS++. Visualization results in Figure 6 further demonstrate that our ScalingConcept method delivers superior concept removal effects. Notably, while LEDITS++ uses a mask to constrain the editing area, this technique can also be incorporated into our method to achieve better region-specific control.

4.3 ABLATION STUDIES

In Table 2, we analyze the trade-off between fidelity and generation quality by varying the value of γ and introducing noise regularization. We set $\omega_{base} = 5$ for all the ablations. The CLIP score for all variants remains similar (28.5 - 28.7), which demonstrates that ω_{base} effectively controls the strength of concept scaling. Overall, our goal is to achieve a better balance between concept scaling and content preservation.

Effect of Different γ . As we gradually increase γ , the FID score rises, indicating that the generated results are shifting from pure generation to a balance between preserving the original content and enhancing the concept (as reflected by the corresponding improvement in the LPIPS score). In this work, we aim to scale the concept, with a focus on achieving a better balance between these factors. Therefore, we select a relatively large value for γ , such as 3.

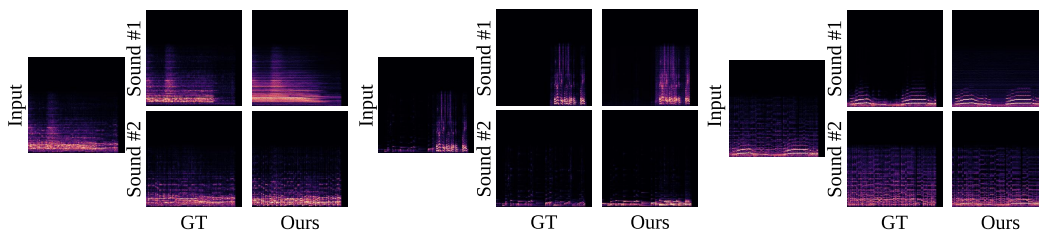
Effect of Noise Regularization and Early Exit. Introducing the noise regularization term into the method significantly improves the LPIPS score from 0.324 to 0.260, indicating better preservation of the original content. However, this introduces a constraint on concept enhancement. When incorporating early exit, both the FID and CLIP scores improve, while content preservation is slightly compromised, leading to a better overall balance.

4.4 ZERO-SHOT APPLICATIONS WITH SCALINGCONCEPT

Our method provides continuous concept scaling up or down for real inputs, making it applicable to a variety of real-world applications. In the audio domain, the continuous scaling capability enables



503 Figure 7: **Applications of ScalingConcept.** We showcase various zero-shot applications across
 504 image and audio modalities, highlighting the surprising effects of scaling concepts up or down,
 505 including non-trivial tasks like canonical pose generation.



514 Figure 8: Qualitative comparison on sound separation. Our method enables zero-shot sound removal
 515 through a generative model.

518 sound highlighting, as illustrated in Figure 1. This involves increasing the volume of a target sound
 519 by scaling the concept of the corresponding sound category using our approach. Another audio
 520 application is sound separation, achieved through a generative model. In Figure 8, we demonstrate
 521 this by using a mixture of sounds as input and scaling down the concept of a non-target sound
 522 by specifying its class as the inversion prompt. We provide a comparison with the ground truth,
 523 showcasing that our method achieves effective sound removal results. In the image domain, our
 524 method can also perform a variety of tasks, such as manipulating weather conditions and, intriguingly,
 525 adjusting poses, among others. We present a preview of these diverse tasks across different domains in
 526 Figure 7. Additional applications can be explored in the Application Zoo, as detailed in Appendix A.1.

527 5 CONCLUSION AND DISCUSSION

528 We propose ScalingConcept, a zero-shot concept scaling method that focuses on enhancing or
 529 suppressing existing concepts in real input data. Our method allows for user-friendly adjustments
 530 by freely tuning the scaling strength ω_{base} and the scaling schedule γ , to achieve a diverse range
 531 of effects. More importantly, ScalingConcept unlocks a variety of non-trivial applications across
 532 different modalities, including canonical pose generation and sound removal or highlighting. This
 533 approach has the potential to serve as a powerful tool within the growing family of diffusion models.
 534 This new method complements existing diffusion-based editing approaches while introducing new
 535 challenges, particularly in scaling multiple concepts simultaneously and minimizing unintended
 536 effects on other concepts. Existing editing methods have benefited from years of advancements to
 537 address similar challenges, such as incorporating attention control. We expect that future work will
 538 build on these developments to effectively tackle these challenges for ScalingConcept.
 539

REFERENCES

- 540
541
542 Manuel Brack, Felix Friedrich, Katharina Kornmeier, Linoy Tsaban, Patrick Schramowski, Kristian
543 Kersting, and Apolinário Passos. Ledits++: Limitless image editing using text-to-image models.
544 In *Proceedings of the IEEE/CVF Conference on Computer Vision and Pattern Recognition*, pp.
545 8861–8870, 2024.
- 546 Tim Brooks, Aleksander Holynski, and Alexei A Efros. Instructpix2pix: Learning to follow image
547 editing instructions. In *Proceedings of the IEEE/CVF Conference on Computer Vision and Pattern
548 Recognition*, pp. 18392–18402, 2023.
- 549 Tim Brooks, Bill Peebles, Connor Holmes, Will DePue, Yufei Guo, Li Jing, David Schnurr, Joe
550 Taylor, Troy Luhman, Eric Luhman, Clarence Ng, Ricky Wang, and Aditya Ramesh. Video
551 generation models as world simulators. 2024. URL [https://openai.com/research/
552 video-generation-models-as-world-simulators](https://openai.com/research/video-generation-models-as-world-simulators).
553
- 554 Haoxin Chen, Menghan Xia, Yingqing He, Yong Zhang, Xiaodong Cun, Shaoshu Yang, Jinbo Xing,
555 Yaofang Liu, Qifeng Chen, Xintao Wang, Chao Weng, and Ying Shan. Videocrafter1: Open
556 diffusion models for high-quality video generation, 2023.
- 557 Haoxin Chen, Yong Zhang, Xiaodong Cun, Menghan Xia, Xintao Wang, Chao Weng, and Ying
558 Shan. Videocrafter2: Overcoming data limitations for high-quality video diffusion models. In
559 *Proceedings of the IEEE/CVF Conference on Computer Vision and Pattern Recognition*, pp.
560 7310–7320, 2024.
561
- 562 Prafulla Dhariwal and Alexander Nichol. Diffusion models beat gans on image synthesis. *NeurIPS*,
563 34:8780–8794, 2021.
- 564 Patrick Esser, Robin Rombach, and Bjorn Ommer. Taming transformers for high-resolution image
565 synthesis. In *CVPR*, pp. 12873–12883, 2021.
566
- 567 Patrick Esser, Sumith Kulal, Andreas Blattmann, Rahim Entezari, Jonas Müller, Harry Saini, Yam
568 Levi, Dominik Lorenz, Axel Sauer, Frederic Boesel, et al. Scaling rectified flow transformers for
569 high-resolution image synthesis. In *Forty-first International Conference on Machine Learning*,
570 2024.
- 571 Rinon Gal, Yuval Alaluf, Yuval Atzmon, Or Patashnik, Amit H Bermano, Gal Chechik, and Daniel
572 Cohen-Or. An image is worth one word: Personalizing text-to-image generation using textual
573 inversion. *arXiv preprint arXiv:2208.01618*, 2022.
574
- 575 Daniel Garibi, Or Patashnik, Andrey Voynov, Hadar Averbuch-Elor, and Daniel Cohen-Or. Renoise:
576 Real image inversion through iterative noising. *arXiv preprint arXiv:2403.14602*, 2024.
- 577 Deepanway Ghosal, Navonil Majumder, Ambuj Mehrish, and Soujanya Poria. Text-to-audio gener-
578 ation using instruction-tuned llm and latent diffusion model. *arXiv preprint arXiv:2304.13731*,
579 2023.
580
- 581 Yuwei Guo, Ceyuan Yang, Anyi Rao, Yaohui Wang, Yu Qiao, Dahua Lin, and Bo Dai. Animatediff:
582 Animate your personalized text-to-image diffusion models without specific tuning. *arXiv preprint
583 arXiv:2307.04725*, 2023.
- 584 Amir Hertz, Ron Mokady, Jay Tenenbaum, Kfir Aberman, Yael Pritch, and Daniel Cohen-Or. Prompt-
585 to-prompt image editing with cross-attention control. In *ICLR*, 2023.
586
- 587 Martin Heusel, Hubert Ramsauer, Thomas Unterthiner, Bernhard Nessler, and Sepp Hochreiter. Gans
588 trained by a two time-scale update rule converge to a local nash equilibrium. *Advances in neural
589 information processing systems*, 30, 2017.
- 590 Jonathan Ho, Tim Salimans, Alexey Gritsenko, William Chan, Mohammad Norouzi, and David J
591 Fleet. Video diffusion models. *arXiv:2204.03458*, 2022.
592
- 593 Hang Hua, Jing Shi, et al. Finematch: Aspect-based fine-grained image and text mismatch detection
and correction. *arXiv preprint arXiv:2404.14715*, 2024.

- 594 Jiawei Huang, Yi Ren, Rongjie Huang, Dongchao Yang, Zhenhui Ye, Chen Zhang, Jinglin Liu, Xiang
595 Yin, Zejun Ma, and Zhou Zhao. Make-an-audio 2: Temporal-enhanced text-to-audio generation.
596 *arXiv preprint arXiv:2305.18474*, 2023a.
597
- 598 Rongjie Huang, Jiawei Huang, Dongchao Yang, Yi Ren, Luping Liu, Mingze Li, Zhenhui Ye, Jinglin
599 Liu, Xiang Yin, and Zhou Zhao. Make-an-audio: Text-to-audio generation with prompt-enhanced
600 diffusion models. In *ICML*, pp. 13916–13932, 2023b.
- 601 Inbar Huberman-Spiegelglas, Vladimir Kulikov, and Tomer Michaeli. An edit friendly ddpm noise
602 space: Inversion and manipulations. In *Proceedings of the IEEE/CVF Conference on Computer
603 Vision and Pattern Recognition*, pp. 12469–12478, 2024.
604
- 605 Xuan Ju, Ailing Zeng, Yuxuan Bian, Shaoteng Liu, and Qiang Xu. Pnp inversion: Boosting diffusion-
606 based editing with 3 lines of code. *International Conference on Learning Representations (ICLR)*,
607 2024.
- 608 Tero Karras. Progressive growing of gans for improved quality, stability, and variation. *arXiv preprint
609 arXiv:1710.10196*, 2017.
610
- 611 Bahjat Kawar, Shiran Zada, Oran Lang, Omer Tov, Huiwen Chang, Tali Dekel, Inbar Mosseri, and
612 Michal Irani. Imagic: Text-based real image editing with diffusion models. In *Proceedings of the
613 IEEE/CVF Conference on Computer Vision and Pattern Recognition*, pp. 6007–6017, 2023.
614
- 615 Levon Khachatryan, Andranik Movsisyan, Vahram Tadevosyan, Roberto Henschel, Zhangyang Wang,
616 Shant Navasardyan, and Humphrey Shi. Text2video-zero: Text-to-image diffusion models are
617 zero-shot video generators. *arXiv preprint arXiv:2303.13439*, 2023.
- 618 Jaeyeon Kim, Jaeyoon Jung, Jinjoo Lee, and Sang Hoon Woo. Enclap: Combining neural audio codec
619 and audio-text joint embedding for automated audio captioning. *arXiv preprint arXiv:2401.17690*,
620 2024.
621
- 622 Nupur Kumari, Bingliang Zhang, Richard Zhang, Eli Shechtman, and Jun-Yan Zhu. Multi-concept
623 customization of text-to-image diffusion. In *CVPR*, pp. 1931–1941, 2023.
- 624 Tsung-Yi Lin, Michael Maire, Serge Belongie, James Hays, Pietro Perona, Deva Ramanan, Piotr
625 Dollár, and C Lawrence Zitnick. Microsoft coco: Common objects in context. In *ECCV*, pp.
626 740–755, 2014.
627
- 628 Haohe Liu, Zehua Chen, Yi Yuan, Xinhao Mei, Xubo Liu, Danilo P. Mandic, Wenwu Wang, and
629 Mark D. Plumbley. Audioldm: Text-to-audio generation with latent diffusion models. In *ICML*,
630 pp. 21450–21474, 2023a.
- 631 Haohe Liu, Qiao Tian, Yi Yuan, Xubo Liu, Xinhao Mei, Qiuqiang Kong, Yuping Wang, Wenwu
632 Wang, Yuxuan Wang, and Mark D Plumbley. Audioldm 2: Learning holistic audio generation with
633 self-supervised pretraining. *arXiv preprint arXiv:2308.05734*, 2023b.
634
- 635 Shilong Liu, Zhaoyang Zeng, Tianhe Ren, Feng Li, Hao Zhang, Jie Yang, Chunyuan Li, Jianwei
636 Yang, Hang Su, Jun Zhu, et al. Grounding dino: Marrying dino with grounded pre-training for
637 open-set object detection. *arXiv preprint arXiv:2303.05499*, 2023c.
638
- 639 Ron Mokady, Amir Hertz, Kfir Aberman, Yael Pritch, and Daniel Cohen-Or. Null-text inversion for
640 editing real images using guided diffusion models. In *Proceedings of the IEEE/CVF Conference
641 on Computer Vision and Pattern Recognition*, pp. 6038–6047, 2023.
- 642 Alexander Quinn Nichol, Prafulla Dhariwal, Aditya Ramesh, Pranav Shyam, Pamela Mishkin, Bob
643 McGrew, Ilya Sutskever, and Mark Chen. GLIDE: towards photorealistic image generation and
644 editing with text-guided diffusion models. In *ICML*, volume 162, pp. 16784–16804, 2022.
645
- 646 Dustin Podell, Zion English, Kyle Lacey, Andreas Blattmann, Tim Dockhorn, Jonas Müller, Joe
647 Penna, and Robin Rombach. Sdxl: Improving latent diffusion models for high-resolution image
synthesis. *arXiv preprint arXiv:2307.01952*, 2023.

- 648 Alec Radford, Jong Wook Kim, Chris Hallacy, Aditya Ramesh, Gabriel Goh, Sandhini Agarwal,
649 Girish Sastry, Amanda Askell, Pamela Mishkin, Jack Clark, et al. Learning transferable visual
650 models from natural language supervision. In *ICML*, pp. 8748–8763, 2021.
- 651 Colin Raffel, Noam Shazeer, Adam Roberts, Katherine Lee, Sharan Narang, Michael Matena, Yanqi
652 Zhou, Wei Li, and Peter J Liu. Exploring the limits of transfer learning with a unified text-to-text
653 transformer. *The Journal of Machine Learning Research*, 21(1):5485–5551, 2020.
- 654 Aditya Ramesh, Prafulla Dhariwal, Alex Nichol, Casey Chu, and Mark Chen. Hierarchical text-
655 conditional image generation with clip latents. *arXiv preprint arXiv:2204.06125*, 1(2):3, 2022.
- 656 Robin Rombach, Andreas Blattmann, Dominik Lorenz, Patrick Esser, and Björn Ommer. High-
657 resolution image synthesis with latent diffusion models. In *CVPR*, pp. 10684–10695, 2022.
- 658 Nataniel Ruiz, Yuanzhen Li, Varun Jampani, Yael Pritch, Michael Rubinstein, and Kfir Aberman.
659 Dreambooth: Fine tuning text-to-image diffusion models for subject-driven generation. In *CVPR*,
660 pp. 22500–22510, 2023.
- 661 Chitwan Saharia, William Chan, Saurabh Saxena, Lala Li, Jay Whang, Emily L Denton, Kamyar
662 Ghasemipour, Raphael Gontijo Lopes, Burcu Karagol Ayan, Tim Salimans, et al. Photorealistic
663 text-to-image diffusion models with deep language understanding. *NeurIPS*, 35:36479–36494,
664 2022.
- 665 Chenyang Si, Ziqi Huang, Yuming Jiang, and Ziwei Liu. Freeu: Free lunch in diffusion u-net.
666 In *Proceedings of the IEEE/CVF Conference on Computer Vision and Pattern Recognition*, pp.
667 4733–4743, 2024.
- 668 Uriel Singer, Adam Polyak, Thomas Hayes, Xi Yin, Jie An, Songyang Zhang, Qiyuan Hu, Harry
669 Yang, Oron Ashual, Oran Gafni, Devi Parikh, Sonal Gupta, and Yaniv Taigman. Make-a-video:
670 Text-to-video generation without text-video data. In *ICLR*, 2023.
- 671 Jascha Sohl-Dickstein, Eric Weiss, Niru Maheswaranathan, and Surya Ganguli. Deep unsupervised
672 learning using nonequilibrium thermodynamics. In *International conference on machine learning*,
673 pp. 2256–2265. PMLR, 2015.
- 674 Jiaming Song, Chenlin Meng, and Stefano Ermon. Denoising diffusion implicit models. In *ICLR*,
675 2020.
- 676 Yunlong Tang, Gen Zhan, Li Yang, Yiting Liao, and Chenliang Xu. Cardiff: Video salient ob-
677 ject ranking chain of thought reasoning for saliency prediction with diffusion. *arXiv preprint*
678 *arXiv:2408.12009*, 2024.
- 679 Yapeng Tian, Jing Shi, Bochen Li, Zhiyao Duan, and Chenliang Xu. Audio-visual event localization
680 in unconstrained videos. In *ECCV*, pp. 247–263, 2018.
- 681 Jay Zhangjie Wu, Yixiao Ge, Xintao Wang, Weixian Lei, Yuchao Gu, Wynne Hsu, Ying Shan,
682 Xiaohu Qie, and Mike Zheng Shou. Tune-a-video: One-shot tuning of image diffusion models for
683 text-to-video generation. *arXiv preprint arXiv:2212.11565*, 2022.
- 684 Weihao Xia, Yulun Zhang, Yujiu Yang, Jing-Hao Xue, Bolei Zhou, and Ming-Hsuan Yang. Gan
685 inversion: A survey. *IEEE TPAMI*, 45(3):3121–3138, 2022.
- 686 Sihan Xu, Yidong Huang, Jiayi Pan, Ziqiao Ma, and Joyce Chai. Inversion-free image editing with
687 natural language. *arXiv preprint arXiv:2312.04965*, 2023.
- 688 Dongchao Yang, Jianwei Yu, Helin Wang, Wen Wang, Chao Weng, Yuexian Zou, and Dong Yu.
689 Diffsound: Discrete diffusion model for text-to-sound generation. *IEEE/ACM Transactions on*
690 *Audio, Speech, and Language Processing*, 2023.
- 691 Yongsheng Yu et al. Promptfix: You prompt and we fix the photo. *arXiv preprint arXiv:2405.16785*,
692 2024.
- 693 Richard Zhang, Phillip Isola, Alexei A Efros, Eli Shechtman, and Oliver Wang. The unreasonable
694 effectiveness of deep features as a perceptual metric. In *Proceedings of the IEEE conference on*
695 *computer vision and pattern recognition*, pp. 586–595, 2018.

A APPENDIX

A.1 APPLICATION ZOO

In this section, we present the application zoo, demonstrating several applications enabled by our ScalingConcept method. Notably, all results are achieved in a zero-shot manner, highlighting the versatility and value of our approach. Additionally, these applications are non-trivial and span across both image and audio domains. For image tasks, we use SDXL Podell et al. (2023) as our base model, while for audio tasks, we employ AudioLDM 2 (Liu et al., 2023b).

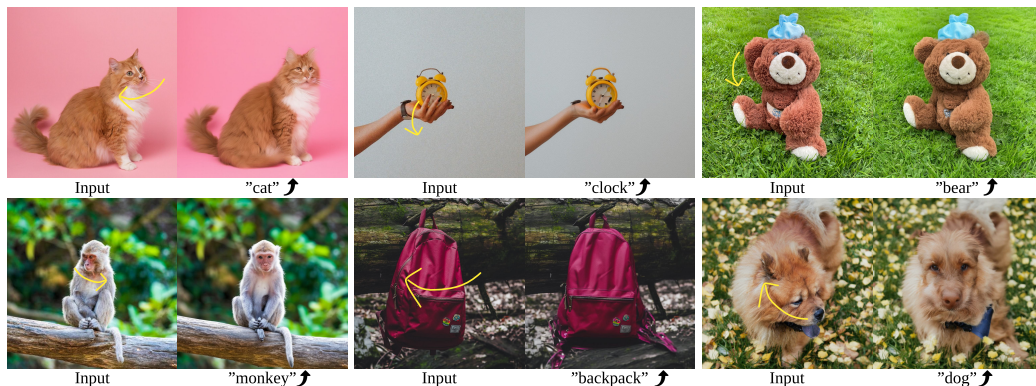


Figure 9: Canonical pose generation. By scaling up the concept of an object, our model adjusts its pose to be more complete and visible.

Canonical pose generation. We identify an interesting and non-trivial task enabled by our ScalingConcept method — adjusting the pose of the subject in the image by scaling up the concept. In Figure 9, we demonstrate the canonical pose generation effect. In the original input images, the concepts to be scaled up, such as the cat, clock, and backpack, are depicted in different poses. After applying concept scaling, the cat and backpack are adjusted to face forward, and the clock’s occlusion by a hand is mitigated, resulting in a more complete expression of the concept. Across all results, scaling up the concept enables seamless and faithful pose adjustments, a task that is challenging even in the 3D domain, yet is effectively addressed by our method. From a high-level perspective, scaling up the concept strengthens its completeness and visibility, often resulting in front-facing orientations. This technique has potential applications in 3D tasks such as novel-view synthesis.

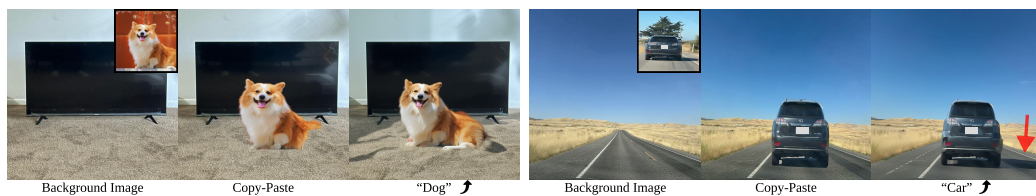


Figure 10: Object stitching. By enhancing an object’s concept, we successfully stitch the object and the background together, completing and harmonizing the whole image.

Object stitching. Another straightforward application is object stitching. When we copy and paste an object into a background image, we scale up the concept in the copy-paste image, which results in making the object more complete. For example, this can be seen in Figure 10, where the dog is completed, the lighting is adjusted, and the shadow of the car is added.

Creative Enhancement. A more open-ended application, as shown in Figure 11, is creative enhancement. In this case, the effect of scaling up the concept is dependent on the actual content of the image, often producing surprising “growing” effects. For example, when scaling up the concept, the “couple” transitions from standing separately to holding hands; and the “pizza” gains additional toppings. This application is particularly useful when users have an arbitrary image and want to enhance the concept to explore different effects.

Weather Manipulation. Since our method supports both scaling up and down concepts, a practical application is weather manipulation (as shown in Figure 12). Scaling down corresponds to classic



770 Figure 11: Creative enhancement. ScalingConcept surprisingly produces “growing” effects based on
771 the content of input images.



781 Figure 12: Weather manipulation. Our method enables both weather suppression, similar to deraining
782 and dehazing tasks, and weather enhancement.

783
784
785 weather mitigation tasks, such as deraining or dehazing, while scaling up the weather is useful in
786 scenarios such as movie production, where specific weather conditions are needed. For example, in
787 the movie “The Mist”, there is no need to wait for naturally heavy fog—our method can faithfully
788 enhance the fog to achieve the desired effect.



801 Figure 13: The top row shows screenshots from the anime “Arknights” (Left) and “Blue archive”
802 (Middle & Right). The bottom row displays the images after scaling up the “anime” concept, which
803 mitigates the fuzziness and blurriness issues commonly encountered in the anime production process.
804

805 **Anime Sketch Enhancement.** During the photography and post-production stages of anime making,
806 cumulative errors in line processing often result in blurred lines, making the image appear fuzzy.
807 Filters for scenes like sunsets exacerbate this issue, which cannot be resolved simply by increasing
808 the resolution or bitrate of the anime. Using our ScalingConcept method, we process images with
809 such issues by applying “anime” as the concept to scale up. This enhances the sketches in the image
as shown in Fig. 13, leading to an overall improvement in visual clarity.

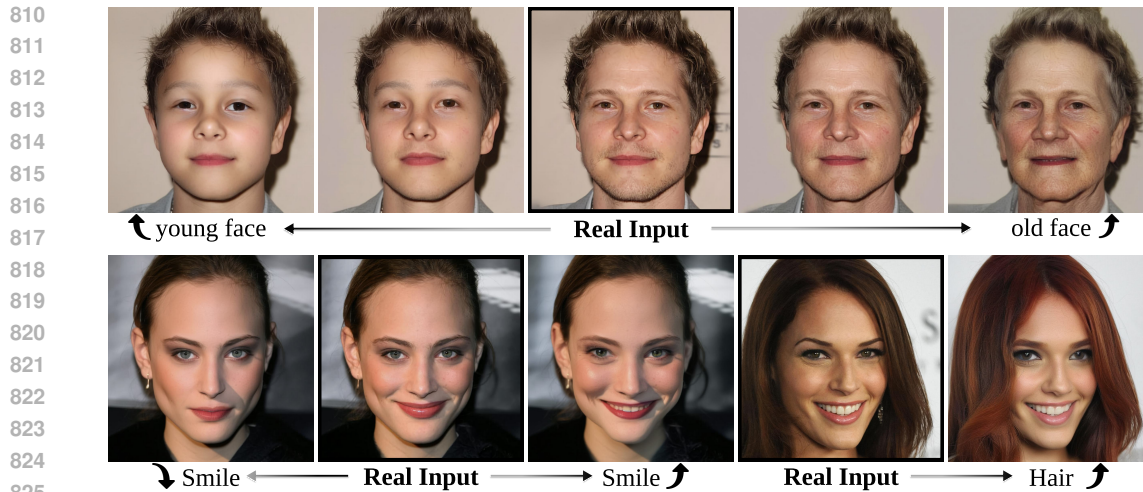


Figure 14: We present a random batch of 3 samples from CelebA-HQ Karras (2017), without cherry-picking, to demonstrate our method’s versatility in scaling different face attribute concepts.

Face Attribute Scaling. We extend our method to face images. In Figure 14, we showcase popular face attribute editing tasks on examples from the CelebA-HQ Karras (2017) dataset, such as adjusting age, smile, and hair. Each of these edits can be achieved by scaling the corresponding concepts, demonstrating the versatility of our method.

A.2 IS CANONICAL POSE GENERATION EASY TO ACHIEVE?



Figure 15: Given the canonical pose generation effect, we attempt to use Instruction Pix2Pix and LEDITS++ to achieve similar results; however, both approaches failed, demonstrating the challenge of this task.

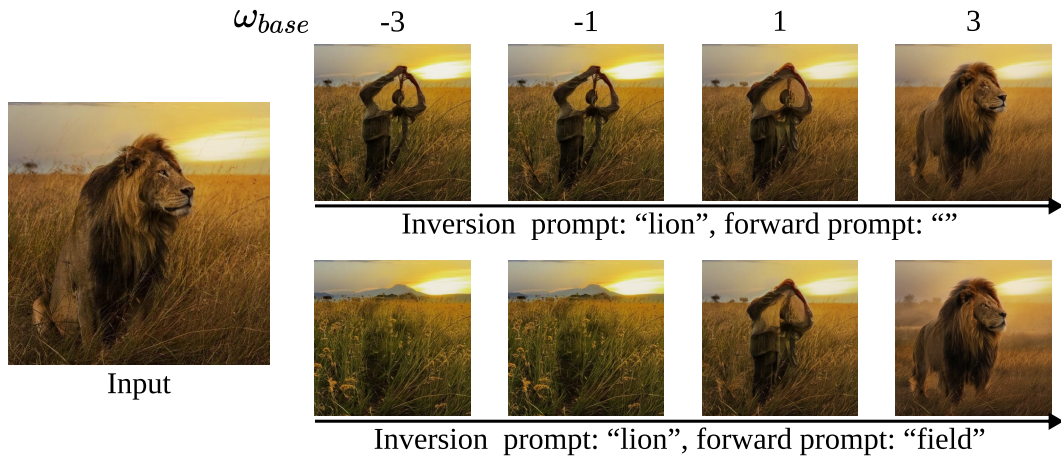
As demonstrated in Fig. 9, our ScalingConcept method can achieve surprising canonical pose generation effects. To further investigate the difficulty of this task, we employ two popular image editing methods: Instruct Pix2Pix Brooks et al. (2023), which follows instructions for editing, and LEDITS++, which adds or removes concepts from the input. Specifically, we instruct Instruct Pix2Pix to “turn the monkey’s head forward,” but the method fails to produce the desired effect. Similarly, when attempting to add the same concept to the input, LEDITS++ does not achieve the pose generation effect, indicating that this task is non-trivial.



877 Figure 16: Visualization of ablation studies. We present the results of concept scaling with different
878 method variants.

880 A.3 VISUALIZATION OF ABLATION STUDIES

882 To illustrate the effects of different components of our method, we visualize the results in Fig. 16,
883 which scales up the concepts of “cat” and “fruits” with $\omega_{base} = 5$. The results demonstrate that our
884 non-linear schedule achieves a better trade-off between fidelity and content preservation. Moreover,
885 adding noise regularization helps preserve more fine-grained details, while the introduction of early
886 exit further improves the trade-off.



903 Figure 17: We set $\gamma = 3$ and vary ω_{base} to investigate its effect. Additionally, we change the prompt
904 from \emptyset to “field” to examine the impact of the forward prompt.

906 A.4 EFFECT OF ω_{base}

908 In the previous experiments, we fix ω_{base} to investigate the effectiveness of other components. In
909 Fig. 17, we showcase the effects of varying ω_{base} , with values ranging from -3 to 3, while fixing
910 $\gamma = 3$. The figure demonstrates that reducing ω_{base} corresponds to the removal of the concept,
911 whereas increasing it enhances the concept. However, we found that the removal effect is not as
912 satisfactory as the enhancement, which highlights a limitation related to text-to-image association.

914 A.5 DOES FORWARD PROMPT MATTER?

915
916 In Fig. 17, changing the forward prompt from \emptyset to “field,” another concept present in the original
917 input, improves the removal effect, as the region left by the null prompt is inpainted with the concept
of “field.” This demonstrates the importance of selecting the correct concept to serve as the removal

918 helper. However, this approach requires additional effort to label the concepts instead of simply
 919 using the versatile null prompt. This suggests an advanced setting for the method, where providing
 920 coarse-level annotations for an additional concept can lead to significant improvements.
 921



936 Figure 18: Overview of the WeakConcept-10 dataset. The images exhibit weak and incomplete
 937 representations of the target concepts, making them ideal candidates for testing concept scaling
 938 methods.
 939

942 A.6 DATASET DETAILS

943 We provide a visualization of the images in our generated WeakConcept-10 dataset in Figure 18.
 944 These generated images exhibit indistinct structures and missing details of the specified concepts,
 945 making them ideal candidates for improvement through concept scaling.
 946

947 For experiments involving concept scaling down on TEDBench, we select one concept from each
 948 image as the scaling-down candidate. The mapping of images to their corresponding concepts is
 949 detailed in Table 3, covering a diverse range of concepts.
 950

951 A.7 LIMITATIONS AND FUTURE WORKS

952 Despite our method presenting a zero-shot approach to scaling concepts in real inputs and achieving
 953 promising results, there are several limitations to the current method.
 954

955 **Choice of Hyperparameters.** In our current method, we split the scaling factor ω_t into two
 956 controlling factors: ω_{base} and the schedule $\beta(t) = (\frac{t}{T})^\gamma$. Users can adjust ω_{base} and γ to control
 957 the scaling strength. Although we demonstrate the effects of different components in Table 2, the
 958 optimal combination varies depending on the task, making user input non-trivial. To address this, a
 959 potential future direction is to design an automatic scaling factor that adapts to the target concept’s
 960 strength, thus eliminating the need for extensive hyperparameter tuning.

961 **Dependence on Text-to-X Association.** While our method enables concept scaling with text-guided
 962 diffusion models for any modality (X), its effectiveness relies heavily on the text-to-X association. If
 963 the text prompt is not sensitive to the diffusion model – meaning the information about the concept is
 964 not captured effectively – the method may fail. To address this issue, incorporating concept-specific
 965 fine-tuning may be beneficial for certain edge cases.
 966
967
968
969
970
971

972
973
974
975
976
977
978
979
980
981
982
983
984
985
986
987
988
989
990
991
992
993
994
995
996
997
998
999
1000
1001
1002
1003
1004
1005
1006
1007
1008
1009
1010
1011
1012
1013
1014
1015
1016
1017
1018
1019
1020
1021
1022
1023
1024
1025

Image File	Concept to be Scaled Down
teddy_1.jpeg	teddy bear
flamingo.jpeg	beach
dog_with_shirt.jpg	shirt
cake_1.jpeg	chocolate shavings
chibi.jpeg	cat
zebra.jpeg	stripes
cat_3.jpeg	cat
empty_street.jpeg	Concrete barriers
couple_beach.jpeg	couple
bird.jpeg	wood
dog_01.jpeg	sand
white_horse2.png	horse
road1.png	road
new_cat_3.jpeg	Long fur
bird-g83440b9c4_1920.jpg	rope
black_shirt.jpeg	watch
milk_cookie.jpeg	milk
door.jpeg	door
giraffe.jpeg	giraffe
goat_and_cat.jpg	cat
elephant.jpeg	elephant
bear3.jpeg	bear
two_dogs_with_checkedered_shirts1.jpg	checkedered hoodies
drinking_horse.png	horse
tennis_ball.jpeg	ball
bird.png	beak
egg_tree.jpeg	Nest
prague.png	building
banana_1.jpeg	banana
dog2_standing.png	Green grass
chair_1.jpeg	chair
box.jpeg	knives
tree_1.jpeg	tree
cat.jpeg	cat
vase_01.jpeg	flowers
apples.jpeg	apples
open_book.jpeg	book
white_horse1.png	horse
red_car.jpeg	Black top
pizza1.png	Red pepper

Table 3: Mapping between image files and the concepts to be scaled down.